THE JOURNAL OF PHYSICAL CHEMISTRY A
A JOURNAL OF THE AMERICAN CHEMICAL SOCIETY

pubs.acs.org/JPCA Article

Kelvin Probe Method to Evaluate Polarization Properties of Liquids

Haruto Jibiki,* Masato Suzuki, Masahiro Ohara, and Hisao Ishii*

Cite This: J. Phys. Chem. A 2025, 129, 2812−2821 Read Online

ACCESS | Metrics & More | Article Recommendations

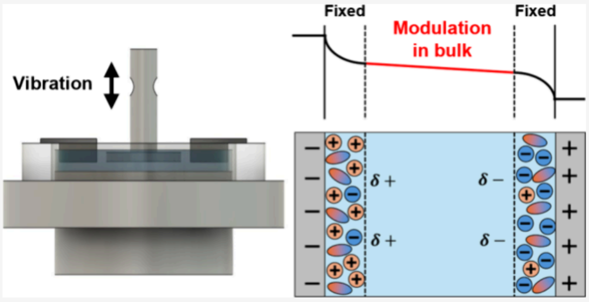

ABSTRACT: The polarization behavior analysis within dielectric materials is crucial for electronics. Here, we reconsidered the Kelvin probe (KP) technique, a widely used method for determining the work function and surface potential of solid materials, for assessing the polarization properties of deformable materials. Unlike impedance spectroscopy (IS), the KP technique measures displacement current by modulating the electrode spacing, rather than electrode potential. By phase-separating KP signal into displacement current and its delayed component (actual current), the KP method is expected to selectively measure polarization properties within the bulk, as the potential drop in the bulk and interface remains constant. We achieved precise phase separation of the KP signal using an optical lever signal synchronized with the electrode vibration as the reference for the lock-in amplifier. The complex dielectric constants $\varepsilon^*_{\mathrm{r,\,KP}}$ and $\varepsilon^*_{\mathrm{r,\,IS}}$ of liquid samples were measured by KP and IS measurement, respectively. For nonpolar octane, $\varepsilon^*_{\mathrm{r,\,KP}}$ was almost equal to $\varepsilon^*_{\mathrm{r,\,IS}}$. Alternatively, for polar 1-octanol and 2-octanol, $\varepsilon^*_{\mathrm{r,\,KP}}$ was smaller than $\varepsilon^*_{\mathrm{r,\,IS}}$. We also estimated that the bulk potential drop in 1-octanol and 2-octanol is approximately one-tenth of the total potential drop. The proposed approach offers a novel method for evaluating energy diagrams and provides insights into the polarization mechanisms of deformable materials.

■ INTRODUCTION

In dielectric materials, an external electric field triggers charge rearrangement and electric dipole rotation, resulting in dielectric polarization. This induced charge distribution finds application across various electronic devices, including capacitors and transistors.[1,2] To evaluate this electric polarization property, several electrical measurement techniques are employed. Among them, impedance spectroscopy (IS) is a widely used method for kinetic analysis, sweeping the modulation frequency of electrode potential. However, IS faces limitations in separately evaluating the bulk and interface responses, as modulation of the electrode potential often triggers interface responses alongside changes in the bulk region. Therefore, there is a need for an alternative measurement method that can suppress interface responses.

We focused on the Kelvin Probe (KP) method as a novel approach for evaluating polarization. In general, KP has been used to measure the work function or surface potential of solid materials. In the KP method, a reference electrode (work function is Φ_R) facing a sample electrode (work function is Φ_S) is vibrated, inducing a displacement current proportional to the difference in Φ_R and Φ_S. This current $I_{KP}(t)$ can be expressed as follows.

$$I_{KP}(t) = \frac{\partial C(t)}{\partial t}(V_{ex} - V_{CPD}) \tag{1}$$

where C, V_{CPD} and V_{ex} represent the capacitance modulated by vibration, the contact potential difference ($V_{CPD} = (\Phi_S - \Phi_R)/e$), and the external bias voltage applied between the sample and reference electrodes, respectively. V_{CPD} is obtained by adjusting V_{ex} to cancel $I_{KP}(t)$. Considering the electric field E, eq 1 can also be expressed as follows.

$$I_{KP}(t) = \frac{\partial D(t)}{\partial t}A = \varepsilon_0 \frac{\partial E(t)}{\partial t}A \tag{2}$$

where D, A and ε_0 denote the electric flux density, the electrode area and the dielectric constant of vacuum, respectively. Typically, KP measurements are conducted in air or vacuum, hence, I_{KP} is proportional to the dielectric constant of vacuum ε_0 (the dielectric constant of air is almost equal to that of vacuum). Initially, this proportionality might seem uninformative for polarization evaluation. If the electrode gap is occupied by a deformable dielectric material, such as a liquid, gel, sol, or elastomer, this proportionality acquires crucial significance. In such scenarios, the signal current can be expressed as follows.

Received: December 20, 2024
Revised: February 19, 2025
Accepted: February 27, 2025
Published: March 5, 2025

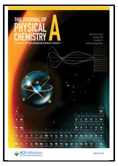

$$I_{\mathrm{KP}}(t) = \varepsilon_{\mathrm{r}}^{*}\varepsilon_0 \frac{\partial E(t)}{\partial t} A = (\varepsilon_{\mathrm{r}}' - j\varepsilon_{\mathrm{r}}'')\varepsilon_0 \frac{\partial E(t)}{\partial t} A \tag{3}$$

where $\varepsilon_{\mathrm{r}}^{*}$ is the complex relative dielectric constant of the dielectric material. Using the proportionality ($I_{\mathrm{KP}}(t) \propto \varepsilon_{\mathrm{r}}^{*}$), the KP method can measure polarization properties without modulating the electrode potential, unlike IS, which necessitates voltage modulation. The signal current in IS measurements can be expressed in the same way as follows.

$$I_{\mathrm{IS}}(t) = C^{*}\frac{\partial V(t)}{\partial t} = \varepsilon_{\mathrm{r}}^{*}\varepsilon_0 \frac{\partial E(t)}{\partial t} A = (\varepsilon_{\mathrm{r}}' - j\varepsilon_{\mathrm{r}}'')\varepsilon_0 \frac{\partial E(t)}{\partial t} A \tag{4}$$

where C^{*} is the complex capacitance. Unlike IS measurements, the classical KP method does not phase-separate the signal current into displacement current ($\propto\varepsilon_{\mathrm{r}}'$) and actual current ($\propto\varepsilon_{\mathrm{r}}''$). For accurate polarization evaluation, the classic KP method requires enhancement to enable phase separation. Therefore, we developed a novel KP system capable of phase-separating the KP signal current.

The fundamental distinction between KP and IS methods lies in how they modulate the electric field: KP modulates the distance between electrodes, while IS modulates the potential difference. The distance modulation in the KP method is expected to selectively measure the bulk response, as it maintains a constant potential drop across the bulk and the interface, minimizing space charge effects at the interface. This is particularly advantageous when dealing with liquids, allowing for the bulk response to be measured while suppressing charging and discharging of the electric double layer (EDL) near the electrodes. Understanding the polarization phenomena at the interface and in the bulk is paramount for liquid-based devices, such as light-emitting electrochemical cell,[3,4] EDL capacitors,[5−7] EDL transistors[8,9] and liquid organic light-emitting diodes.[10−12]

Previous attempts to apply the KP method in liquids have primarily focused on work function changes and surface potential in liquids.[13−17] However, the use of KP as a method for evaluating the polarization properties of liquids has not yet been fully explored. Recently, Kelvin Probe Force Microscopy (KPFM), which is capable of imaging surface potential, has also been employed in liquids to measure surface potential and charge distribution.[18−24] While KPFM can assess the dielectric properties of the scanning surface,[25−29] KPFM is not well-suited for quantitative evaluation of polarization properties between the electrodes because of two significant challenges: (i) potential modulation is required to generate electrostatic force signal, and (ii) the electrode areas of the capacitor between the scanning tip and the sample are geometrically asymmetric, resulting in a nonuniform electric field. Therefore, the KP method is more effective than KPFM for evaluating polarization properties between electrodes, such as those assessed by IS measurements.

In this study, we have developed a phase-separated KP system. In this system, the optical lever signal, reflecting the probe electrode vibration, serves as the reference signal for the lock-in amplifier (LIA) to detect the KP signal. This approach enables high-precision phase separation, unaffected by vibration phase shifts caused by liquid viscosity. Using this system, we investigated the potential of the KP method as a polarization evaluation tool. To compare KP and IS, we measured two complex dielectric constants, $\varepsilon_{\mathrm{r,\,KP}}^{*}$ and $\varepsilon_{\mathrm{r,\,IS}}^{*}$, using KP and IS measurements, respectively. For a nonpolar liquid octane, the two dielectric constants were almost equal. Alternatively, for polar liquids 1-octanol and 2-octanol, real part $\varepsilon_{\mathrm{r,\,KP}}'$ was clearly smaller than $\varepsilon_{\mathrm{r,\,IS}}'$. This reduction in $\varepsilon_{\mathrm{r,\,KP}}'$ can be ascribed to the screening of the bulk electric field by space charge at the interface. By analyzing the difference between the two dielectric constants, we evaluated bulk potential drop in octane, 1-octanol, and 2-octanol, suggesting the feasibility of the KP method for evaluating potential profiles in liquid devices.

■ THEORETICAL AND EXPERIMENTAL METHODS

KP is a method employed to measure the work function or surface potential of solid materials. During a KP measurement, the reference electrode, positioned facing the sample electrode undergoes vibrations. This modulation results in a variation of the distance d between the two electrodes, expressed mathematically as follows.

$$d(t) = d_0 + d_1 e^{j\omega t} \tag{5}$$

where ω, d_0 and d_1 represent the angular frequency, the mean electrode spacing and the amplitude of the electrode vibration, respectively. This vibration modulates the electric field E. Assuming that d_1 is sufficiently smaller than d_0, the electric field can be expressed as follows.

$$E(t) = \frac{V}{d(t)} = \frac{V_{\mathrm{CPD}} - V_{\mathrm{ex}}}{d_0 + d_1 e^{j\omega t}} \approx \frac{V_{\mathrm{CPD}} - V_{\mathrm{ex}}}{d_0}\left(1 - \frac{d_1}{d_0}e^{j\omega t}\right) \tag{6}$$

This field modulation produces a displacement current $I_{\mathrm{KP}}(t)$. In air or vacuum, $I_{\mathrm{KP}}(t)$ can be expressed as follows.

$$I_{\mathrm{KP}}(t) = \frac{\partial D}{\partial t} A = \varepsilon_0 \frac{\partial E}{\partial t} A \approx \varepsilon_0 (V_{\mathrm{ex}} - V_{\mathrm{CPD}}) \frac{d_1}{{d_0}^2} A\omega \cdot j e^{j\omega t} \tag{7}$$

This signal current $I_{\mathrm{KP}}(t)$ is proportional to $V_{\mathrm{ex}} - V_{\mathrm{CPD}}$. In the traditional null-detection method, to determine V_{CPD}, V_{ex} was controlled by a feedback loop system so that this signal current cancels out to hold $V_{\mathrm{CPD}} - V_{\mathrm{ex}} = 0$. In off-null operation,[30] the linear relation between V_{ex} and $I_{\mathrm{KP}}(t)$ is measured as shown in Figure 1. V_{CPD} can be determined from the intercept of the linear fit of this plot with the V_{ex} axis. The measurement accuracy of this method surpasses that of the null-detection method, especially in environments with insufficient signal-to-noise ratios. The linear-fitted line gradient, G, serves as a quality factor for the measurement. Typically, G is used to adjust d_0 to achieve a desired signal intensity level. However, this study emphasizes another aspect

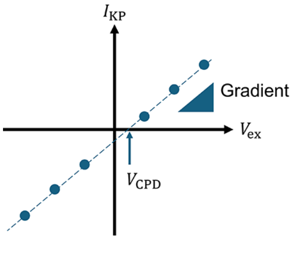

Figure 1. Relation between the external bias (V_{ex}) and current measured in KP (I_{KP}) in the case of off-null operation. The intercept on the horizontal axis corresponds to the contact potential difference (V_{CPD}), and the slope of the line (G) is proportional to the dielectric constant of the sample between the electrodes.

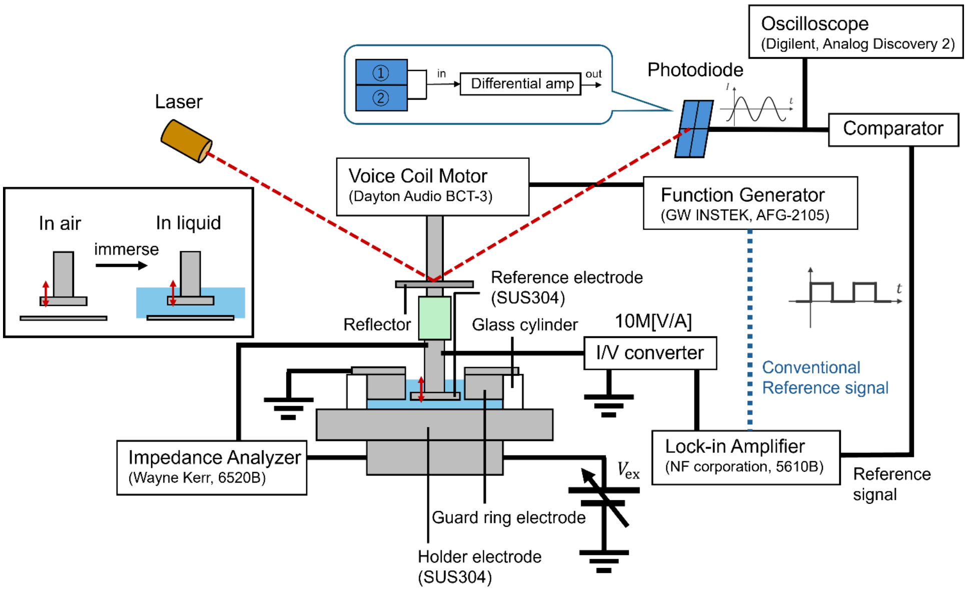

Figure 2. Experimental setup for conducting KP and IS measurements. KP measurement is performed by vibrating the reference electrode immersed in liquid sample. The laser beam is reflected off a mirror attached to the electrode and detected by the photodiode, serving as a reference signal. IS measurement is performed by switching the setup to the impedance analyzer. See the text for the detail.

of G: its proportionality to the dielectric constant of the material placed between the electrodes. This proportionality is particularly significant when the space is occupied by deformable dielectric materials, such as liquids, gels, sols, or elastomers. Under these conditions, the signal current $I_{KP}(t)$ can be expressed as follows.

$$\begin{aligned} I_{KP}(t) &= \frac{\partial D}{\partial t}A \\ &= \varepsilon_r^* \varepsilon_0 \frac{\partial E}{\partial t} A \\ &\approx (V_{ex} - V_{CPD})(\varepsilon_r' - j\varepsilon_r'')\varepsilon_0 \frac{d_1}{d_0{}^2} A\omega \cdot je^{j\omega t} \end{aligned} \tag{8}$$

Thus, the gradient G should offer critical insights into the polarization properties of these dielectric materials.

The signal current in air, $I_{air}(t)$, as expressed in eq 7, and in dielectric material, $I_{di}(t)$, as expressed in eq 8, can also be expressed as follows, respectively.

$$I_{air}(t) = I'_{KP} \cdot je^{j\omega t} \tag{9}$$

$$I_{di}(t) = |I_{KP}| \cdot je^{j(\omega t + \Phi)} = I'_{KP} \cdot je^{j\omega t} + I''_{KP} \cdot e^{j\omega t} \tag{10}$$

where Φ, I'_{KP} and I''_{KP} represent the phase delay derived from the dielectric loss ε_r'', displacement current ($\propto \varepsilon_r'$) and actual current ($\propto \varepsilon_r''$), respectively. $I_{di}(t)$ comprises two components in different phases. By detecting $I_{di}(t)$ with LIA, the DC output signal I_{out} can be expressed as follows.

$$I_{out}(t) = \frac{1}{T} \int_{t-T}^{t} \sin(\omega_r s + \phi) I_{di}(s) \mathrm{d}s \tag{11}$$

where T, ω_r and φ denote the time constant of the LIA, the angular frequency of the reference signal, and the phase offset adjustable on the LIA, respectively. A two-phase LIA provides two signal outputs, X_ω and Y_ω, where Y_ω has an additional 90° phase offset relative to X_ω. In conventional KP measurements, φ is adjusted to maximize either X_ω or Y_ω, providing highly accurate V_{CPD} measurements. However, in dielectric materials, maximizing X_ω is unnecessary; instead, separating X_ω and Y_ω—i.e., I'_{KP} and I''_{KP} —using an appropriate reference phase is crucial. To achieve this, we adopted the optical lever signal reflecting electrode vibration as the reference signal for the LIA, as described later. This signal reflects vibration phase shifts caused by liquid viscosity, providing a reference signal corresponding to the vibration phase under any conditions. Using this reference signal, $I_{di}(t)$ can be phase-separated into I'_{KP} and I''_{KP}. The first step in the phase separation process involves calibrating φ to maximize X_ω for the KP signal in air $I_{air}(t)$. This calibration allows X_ω to represent I'_{KP} and Y_ω to represent I''_{KP}, enabling phase separation of the KP signal even in liquids. This process is necessary because the optical lever signal exhibits a certain phase shift from the actual vibration phase due to the parasitic capacitance of the photodiode. We can then evaluate $\varepsilon^*_{r,\,KP}$ by using gradients G'_{liq} and G''_{liq} determined from I'_{KP} and I''_{KP} in liquids. The dielectric constant $\varepsilon'_{r,\,KP}$ can be determined as follows.

$$\frac{G'_{liq}}{G'_{air}} = \frac{\varepsilon_0 \varepsilon_r'}{\varepsilon_0} = \varepsilon'_{r,KP} \tag{12}$$

The dielectric loss ε_r'' can be also determined in the same way.

$$\frac{G''_{liq}}{G'_{air}} = \frac{\varepsilon_0 \varepsilon_r''}{\varepsilon_0} = \varepsilon''_{r,KP} \tag{13}$$

In IS measurement, $\varepsilon^*_{r,\,IS}$ is determined as follows.

$$\frac{C^*_{liq}}{C_{air}} = \frac{\varepsilon_0 \varepsilon_r^*}{\varepsilon_0} = \varepsilon^*_{r,IS} = \varepsilon'_{r,IS} - j\varepsilon''_{r,IS} \tag{14}$$

where C^*_{liq} and C_{air} are the measured complex capacitance of the cell filled by liquids and the measured capacitance of the cell without liquid, respectively.

https://doi.org/10.1021/acs.jpca.4c08604
J. Phys. Chem. A 2025, 129, 2812−2821

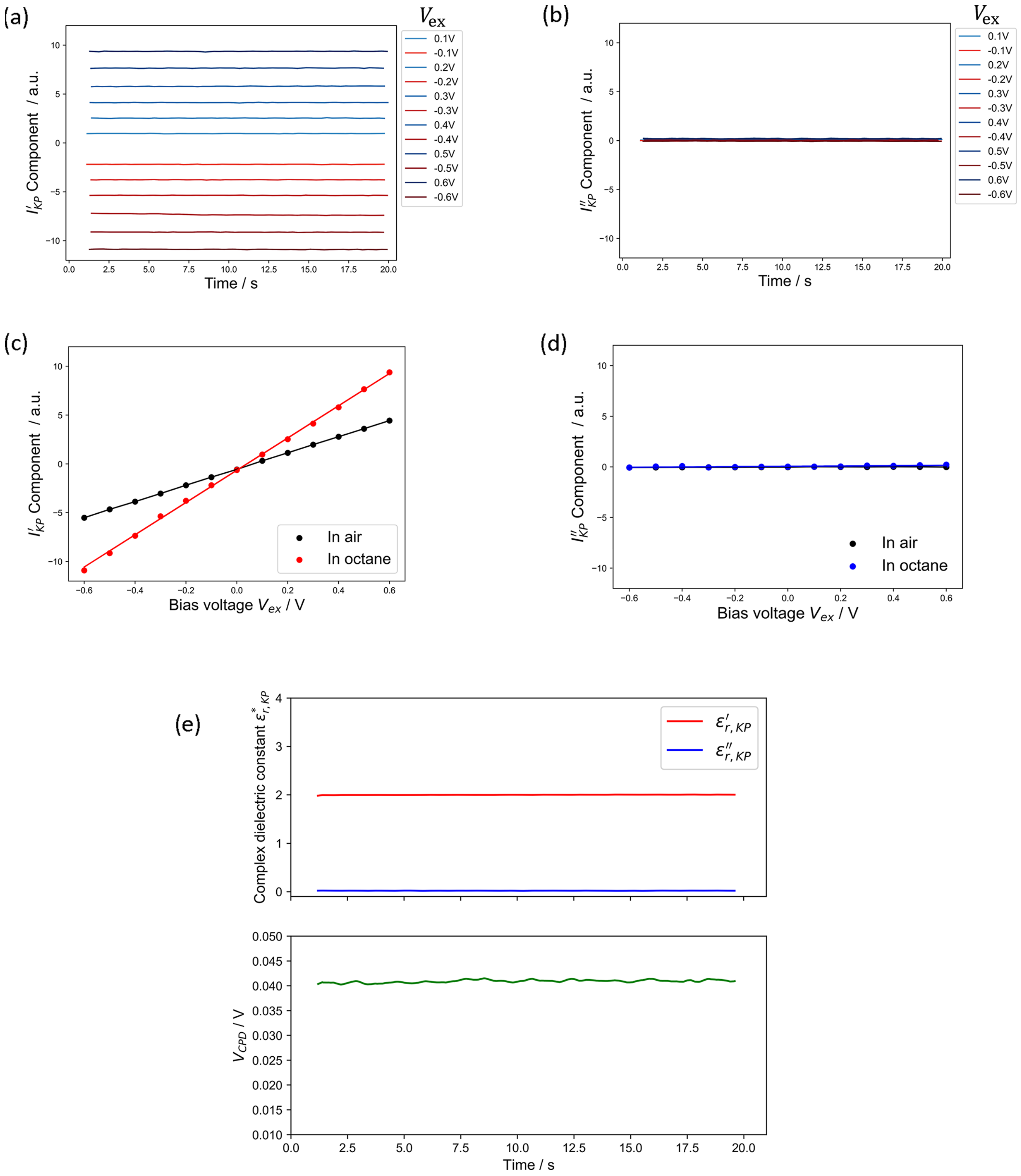

Figure 3. Phase-separated KP results in octane. (a) Time dependence of I'_{KP}, (b) time dependence of I''_{KP}, (c) I'_{KP} plotted on V_{ex}, (d) I''_{KP} plotted on V_{ex}, and (e) time dependences of ε^*_{KP} and V_{CPD}.

■ MEASUREMENT SYSTEM

The experiments were conducted using a homemade measurement system as shown in Figure 2. This system facilitates the measurement of KP and IS in air and liquid, respectively. The disk-shaped reference electrode (8 mm in diameter) can be immersed in the liquid sample contained within the holder electrode. Both electrodes are made of SUS304, a widely used stainless steel alloy, primarily composed of iron (Fe), chromium (Cr, ∼ 18%), and nickel (Ni, ∼ 8%). In the KP setup, the reference electrode was vibrated by a voice coil motor (Dayton Audio BCT-3), while the signal current was measured using LIA (NF corporation, 5610B) through a homemade I/V converter (Gain: 10 M [V/A]). According to the analysis of capacitance and gradient, the mean electrode spacing d_0 and the amplitude of electrode vibration d_1 were approximately 100 and 10 μm, respectively. Both values are significantly larger than the typical thickness of the EDL. An optical lever signal was used as reference signal for LIA instead of the drive voltage of the voice coil motor. This signal was generated by detecting a laser beam reflected from a mirror attached to the vibrating electrode using a split photodiode (Hamamatsu Photonics, S5981). To render this signal suitable for phase detection, it was amplified in differential mode and converted into a stable square wave using a comparator. Additionally, the shifts in d_0 or d_1 due to the liquid's viscosity were manually corrected by adjusting the output driving voltage of the voice coil motor, as monitored by the optical lever signal. A guard ring electrode, maintained at the same potential as the reference electrode, was used to suppress the fringing electric field. For V_{CPD} measurements, the instrumental uncertainty was approximately 3 mV. Using impedance analyzer (Wayne Kerr, 6520B), this system can be configured for IS setup, with the equivalent circuit for capacitance analysis being a parallel circuit consisting of a single resistor and capacitor. Both the electrode vibration in KP and AC voltage in IS were operated at a frequency of 605 Hz. At a relatively low frequency of 605 Hz, non-negligible dielectric loss ε_r'' should contribute to actual current I_{KP}'' in the phase-separated KP measurement. Prior to each experiment, the electrodes were polished with emulsifying liquid metal polish and ultrasonically cleaned twice with detergent, acetone and 2-propanol. The liquid samples used in the experiments were *n*-octane (purity >98%, FUJIFILM Wako Pure Chemical), 1-octanol (purity >99%, Tokyo Chemical Industry), and 2-octanol (purity >98%, Tokyo Chemical Industry).

■ RESULTS

The results of KP measurement for nonpolar *n*-octane are presented in Figure 3. The time dependence of phase-separated KP signals, I_{KP}' and I_{KP}'', after applying the bias voltage V_{ex}, was measured (Figure 3(a) and (b)). As in air, only the time-independent displacement current I_{KP}' was detected. Immediately after the voltage application, a large transient current made detection by the LIA impossible (not shown). When comparing the V_{ex}-dependence of I_{KP}' with that in air, the gradient G_{liq}' in octane was larger than the gradient G_{air}' in air (Figure 3(c)). Conversely, the gradients G_{liq}'' in octane and G_{air}'' of I_{KP}'' in air were nearly zero (Figure 3(d)). Using these converged values, $\varepsilon_{\mathrm{KP}}^*$ and V_{CPD} were determined, as shown in Figure 3(e). These measured values also exhibited no time dependence. As reference results, $\varepsilon_{\mathrm{IS}}^*$ measured using IS measurement under the same setup, the corresponding value reported in literature, and V_{CPD} in air before immersion in octane are provided in Table 1. The values $\varepsilon_{\mathrm{KP}}^*$ and $\varepsilon_{\mathrm{IS}}^*$ were nearly identical, indicating that the dielectric property analysis of nonpolar liquids can be effectively performed using KP, similar to IS. The nonzero V_{CPD} in air is attributed to slight variations in surface conditions of electrodes. In air, surface adsorption of molecules such as water induces a shift in the work function of the two electrodes. The V_{CPD} slightly changed before and after immersion. This change is likely due to the removal of adsorbed molecules (e.g., water) from the electrode surface or the adsorption of the octane. Similar changes was also reported in decane.[21]

Table 1. Measured Complex Dielectric Constants and V_{CPD} (in Air and Octane)

$\varepsilon_{r,\mathrm{KP}}'$	$\varepsilon_{r,\mathrm{IS}}'$	$\varepsilon_{r,\mathrm{KP}}''$	$\varepsilon_{r,\mathrm{IS}}''$	ε_r' (in ref 31)	V_{CPD}/V (In air)	V_{CPD}/V (In octane)
1.99	1.83	0.00	0.00	1.95	0.065	0.038

The results of KP measurements for polar 1-octanol are presented in Figure 4. In 1-octanol, I_{KP}' and the actual current I_{KP}'' were detected, with both currents exhibiting time-decaying signals, as shown in Figure 4(a) and (b). Similar signal decay in ionically active polar liquids has been previously observed in KPFM measurements, attributed to ion diffusion dynamics.[20] However, the prolonged decay observed in this study, which occurs over tens of seconds, is significantly longer than the diffusion time scales reported in the previous study. This prolonged time scale can be attributed to the high viscosity of 1-octanol (7.363 mPa·s)[32] and the longer electrode spacing compared to KPFM, which results in a slower diffusion process. At such long time scales, Faradaic processes, e.g., the reduction of dissolved oxygen, could also contribute to the observed decay. The dependence of these signals on V_{ex} at the time t = 10 and 200 s was compared with the signal in air (Figure 4(c) and (d)). These plots demonstrated nonlinear behavior with respect to V_{ex}, likely due to nonlinear responses associated with electrochemical reactions or diffusion dynamics of ions. However, within the low-voltage range (-0.4 V ≤ V_{ex} ≤ 0.4 V), the signal was relatively linear behavior, suggesting that pure KP signal is dominant. Therefore, the gradient of the plot within this range was used to determine $\varepsilon_{\mathrm{KP}}^*$ and V_{CPD}, as shown in Figure 4(e). The observed changes in $\varepsilon_{\mathrm{KP}}^*$ and V_{CPD}, which were absent in nonpolar liquids like octane, likely reflect the formation of an electric field due to space charge redistribution near the electrodes. The value at t = 200 s was assumed to represent the equilibrium KP results and was compared with reference results (Table. 2). The values of $\varepsilon_{r,\mathrm{IS}}'$ and $\varepsilon_{r,\mathrm{KP}}''$ were significantly smaller than those of $\varepsilon_{r,\mathrm{IS}}'$ and $\varepsilon_{r,\mathrm{IS}}''$, suggesting that in polar liquids, KP measurements evaluate properties distinct from those assessed by IS measurements. Notably, $\varepsilon_{r,\,\mathrm{KP}}'$ was less than 1. A discussion of the reasons for this is given in the following section. Regarding V_{CPD}, its interpretation in 1-octanol may differ from that in octane. The V_{CPD} measured in polar liquids is also discussed later.

The results of KP measurements for another polar liquid, 2-octanol, are presented in Figure 5. The dependence of these signals on V_{ex} at t = 10 and 200 s was compared with the signal in air (Figure 5(a) and (b)). Although I_{KP}' was smaller than I_{KP}'', both components were detected. Similar to 1-octnaol, the signals exhibited time-dependent decay and nonlinear behavior with respect to V_{ex}.

The gradient in the relatively linear region (-0.4 V ≤ V_{ex} ≤ 0.4 V) was used to determine $\varepsilon_{\mathrm{KP}}^*$ and V_{CPD}. The values at t = 200 s were compared with the reference results (Table. 3). As observed in 1-octanol, $\varepsilon_{r,\,\mathrm{KP}}'$ was significantly smaller than $\varepsilon_{r,\,\mathrm{IS}}'$. In contrast, $\varepsilon_{r,\,\mathrm{KP}}''$ was larger than $\varepsilon_{r,\,\mathrm{IS}}''$.

■ DISCUSSION

In the KP measurement for nonpolar octane, the KP signal remained constant over time, and $\varepsilon_{r,\,\mathrm{KP}}^*$ was almost same as the value of $\varepsilon_{r,\,\mathrm{IS}}^*$. In other words, the KP signal can be represented by a simple expression as like in air. Alternatively, for polar 1-octanol and 2-octanol, $\varepsilon_{r,\,\mathrm{KP}}^*$ was clearly smaller than $\varepsilon_{r,\,\mathrm{IS}}^*$. This

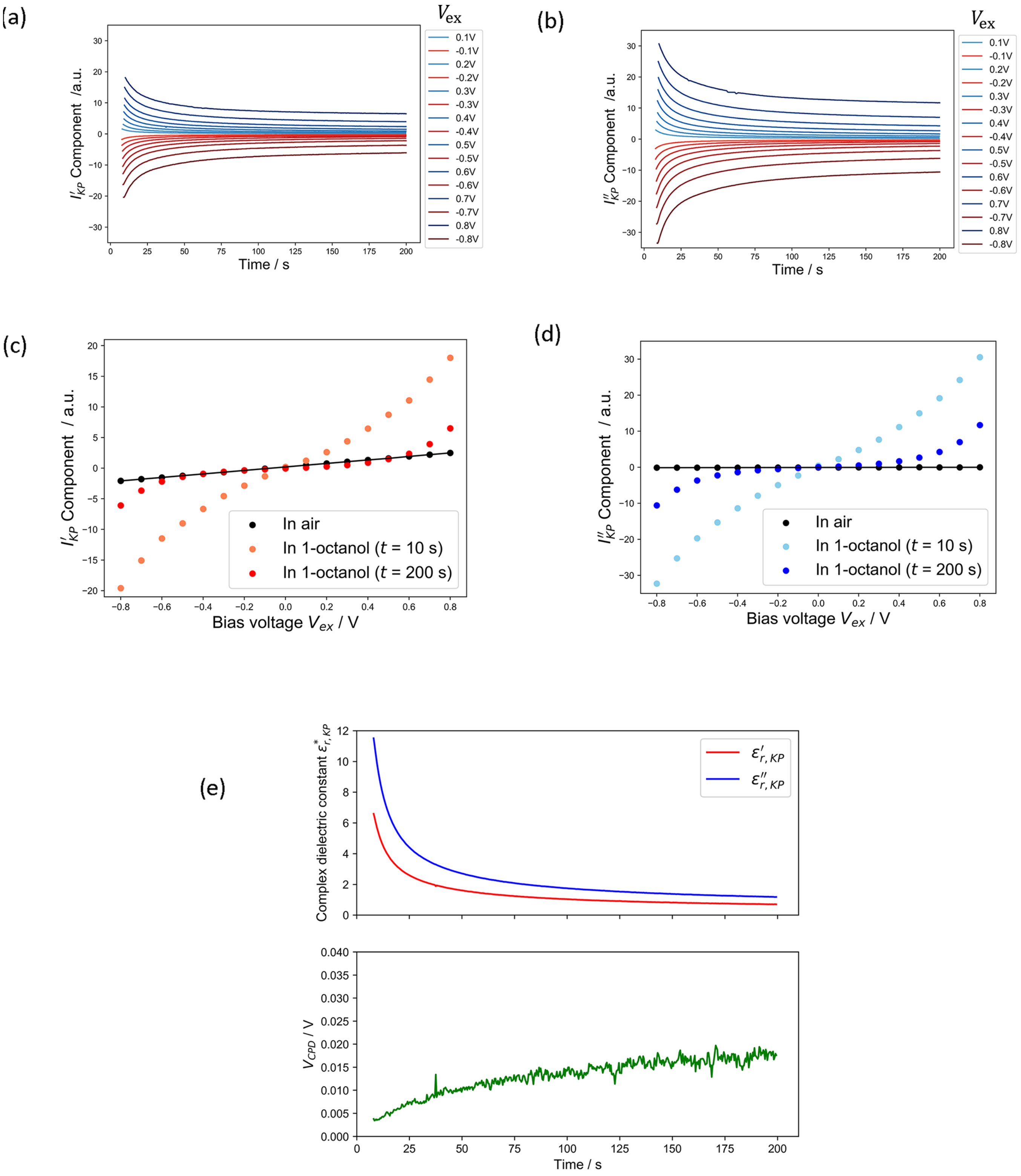

Figure 4. Phase-separated KP results in 1-octanol. (a) Time dependence of I'_{KP}, (b) Time dependence of I''_{KP}, (c) I'_{KP} plotted on V_{ex}, (d) I''_{KP} plotted on V_{ex}, and (e) time dependences of ε^*_{KP} and V_{CPD}.

Table 2. Measured Complex Dielectric Constants and V_{CPD} (in Air and 1-Octanol)

$\varepsilon'_{r,KP}$	$\varepsilon'_{r,IS}$	$\varepsilon''_{r,KP}$	$\varepsilon''_{r,IS}$	ε'_{r}(in ref 33)	V_{CPD}/V (In air)	V_{CPD}/V (In liquid)
0.71	9.23	1.19	79.0	10.39	−0.069	0.018

finding indicates that the KP signal in polar liquids are proportional to the time derivative of the bulk electric field reduced by EDL as described below.

To elucidate the differences between KP and IS measurements, we considered the model illustrated in Figure 6. In polar liquids exposed to air, an external electric field causes

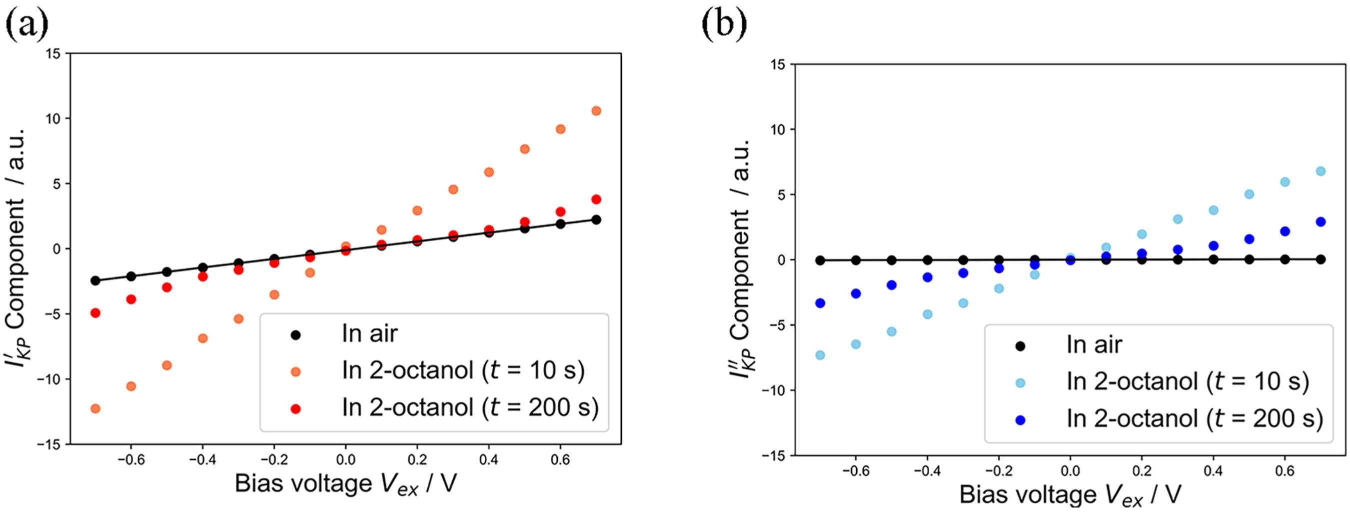

Figure 5. Phase-separated KP results in 2-octanol. (a) I'_{KP} plotted on V_{ex} and (b) I''_{KP} plotted on V_{ex}.

Table 3. Measured Complex Dielectric Constants and V_{CPD} (in Air and 2-Octanol)

$\varepsilon'_{r,KP}$	$\varepsilon'_{r,IS}$	$\varepsilon''_{r,KP}$	$\varepsilon''_{r,IS}$	ε'_r (in ref 33)	V_{CPD}/V (In air)	V_{CPD}/V (In liquid)
1.30	8.40	0.87	0.30	8.68	0.032	0.052

impurity ions (e.g., HCO_3^-) to accumulate near the electrode. Additionally, electric dipoles are expected to strongly orient near the electrode interface. As a result, a space charge is formed at the interface. Within the bulk, liquid molecules are expected to polarize uniformly like a lossless dielectric. In the IS model, the modulation of the electrode potential results in the modulation of electric fields in both the bulk and the interface, accompanied by changes in space charge distributions. By contrast, the KP model assumes that a constant electrode potential fixes the space charge layer at the interface and only the electric field in the bulk is modulated. As a result, the KP signal only reflects the modulation of the electric field in the bulk, which is screened by the space charge layer. Under this assumption, the KP signal current can be expressed as follows.

$$I_{KP} = \varepsilon_0 \varepsilon_r^* \frac{\partial E_{bulk}}{\partial t} A = \frac{\partial C^*}{\partial t} V_{bulk} \tag{15}$$

where E_{bulk} and V_{bulk} are the electric field and potential drop in the bulk, respectively. This equation indicates that the KP signal contains information about V_{bulk}. Regarding V_{CPD} measurement, the V_{CPD} measured in polar liquids is affected by the screening effect of the interfacial space charge. In other words, this measured V_{CPD} reflects an effective work function difference, which includes contributions from the interface. The total potential drop V_{total} between electrodes can be expressed as follows.

$$V_{total} = V_{bulk} + V_{int} \tag{16}$$

where V_{int} is the interface potential drop caused by the space charge layer. For air or nonpolar liquid, V_{int} does not occur since there is no space charge. In this case, V_{total} can be expressed as follows.

$$V_{total} = V_{bulk}(= V_{CPD} - V_{ex}) \tag{17}$$

This equation shows that the region probed by the KP signal is influenced by the presence or absence of a space charge at the interface. This has a substantial impact on determining $\varepsilon'_{r,\,KP}$ as follows.

$$\varepsilon'_{r,KP} = \frac{G'_{di}(\propto \varepsilon_0 \varepsilon_r V_{bulk})}{G'_{air}(\propto \varepsilon_0 V_{total})} = \varepsilon'_{r,IS} \cdot \frac{V_{bulk}}{V_{total}} \tag{18}$$

This equation demonstrates that the reason for the smaller values of $\varepsilon'_{r,\,KP}$ for 1-octanol and 2-octanol is that the bulk potential drop was screened by the interfacial space charge. The apparent dielectric constant $\varepsilon'_{r,\,KP}$ reflects the electric field change in the bulk. Therefore, for polar liquids, IS is more suitable at measuring dielectric constant. However, eq 18 also indicates that comparing $\varepsilon'_{r,\,KP}$ and $\varepsilon'_{r,\,IS}$ reflects the ratio of V_{bulk} to V_{total}. A similar argument may apply to the comparison of $\varepsilon''_{r,\,KP}$ and $\varepsilon''_{r,\,IS}$. However, the measured value may be affected by variations in the contribution of impurity ions between experiments and the influence of slow dynamics induced by electrode vibration in the KP method. Therefore, accurately comparing and discussing $\varepsilon''_{r,\,KP}$ and $\varepsilon''_{r,\,IS}$ remains challenging.

Using Eq. 18, the potential profiles for octane, 1-octanol, and 2-octanol were evaluated and are shown in Figure 7. In nonpolar octane, the agreement between $\varepsilon'_{r,\,KP}$ and $\varepsilon'_{r,\,IS}$ indicates that no interface potential drop occurs. This is consistent with the fact that octane has no dipole moment and is ionically inactive. In contrast, for polar 1-octanol and 2-octanol, $\varepsilon'_{r,\,KP}$ and $\varepsilon'_{r,\,IS}$ were totally different. Comparing these two values reveals that, for both liquids, the value of $\varepsilon'_{r,\,KP}$ is approximately one-tenth of $\varepsilon'_{r,\,IS}$, indicating that V_{bulk} is about one-tenth of V_{total}. The ratio $\varepsilon'_{r,\,KP}/\varepsilon'_{r,\,IS}$, which reflects the bulk potential drop V_{bulk}, was found to be slightly larger in 2-octanol than in 1-octanol. This suggests that the screening effect in 2-octanol is weaker, which could be attributed to its smaller dipole moment or its lower activity toward impurity ions compared to 1-octanol. It is challenging to conclusively determine which factor has a more dominant contribution to screening effect. However, in practical systems, the overall screening effect resulting from both contributions is what ultimately matters. The results of this study demonstrate that the potential drop in the bulk can be effectively evaluated from experimental data, even in polar liquids containing space

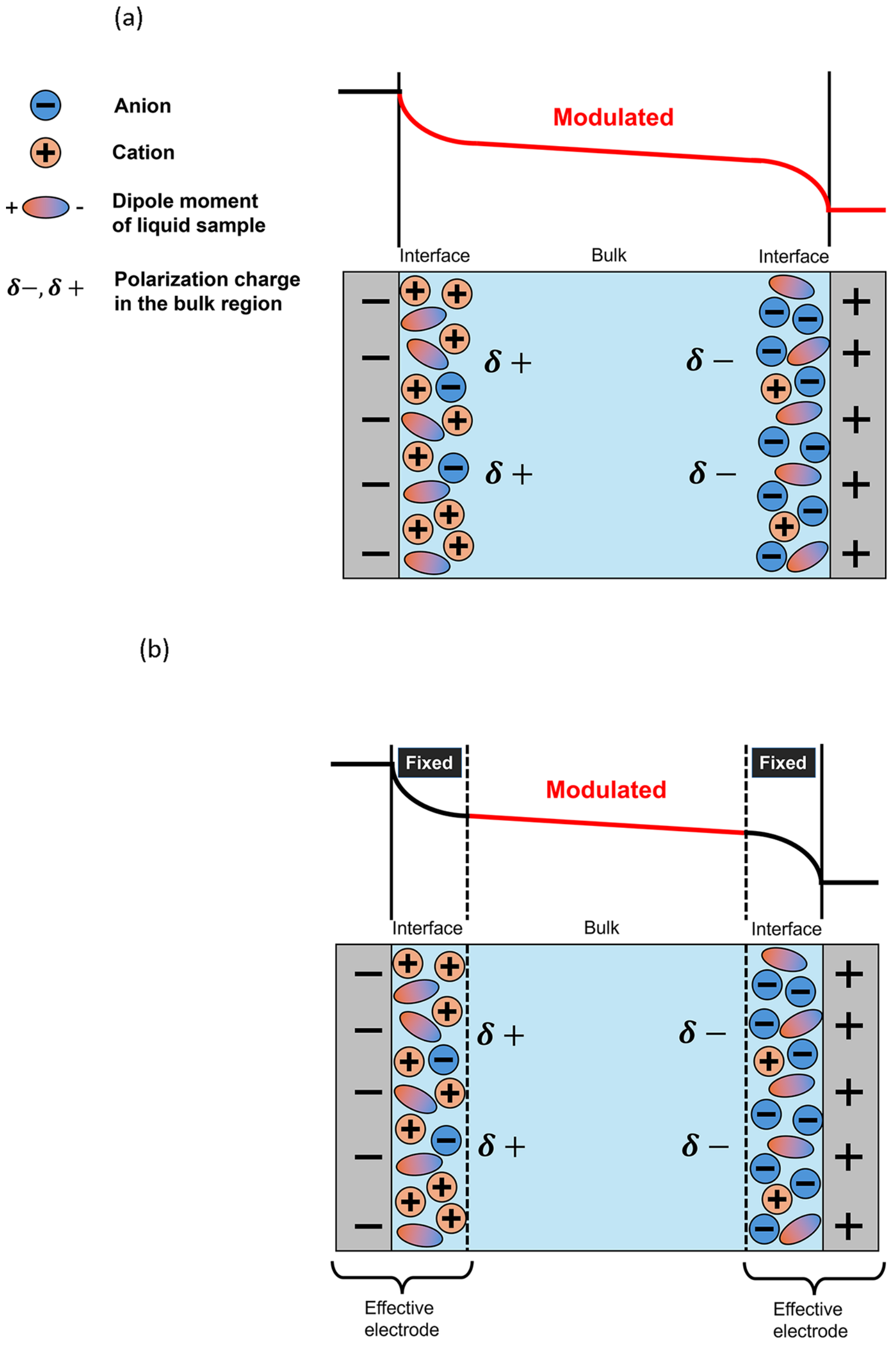

Figure 6. Possible potential profile between the two electrodes during the measurement of (a) IS and (b) KP.

charge. Additionally, we are planning measurements under an inert gas atmosphere to suppress impurities, as well as experiments investigating the effect of added electrolyte concentration.

■ CONCLUSIONS

In this study, the KP method was reconsidered as a tool for analyzing the electric polarization properties of deformable materials. A phase-separated KP system was developed, using an optical lever signal. The two complex dielectric constants $\varepsilon^*_{\mathrm{r,\,KP}}$ and $\varepsilon^*_{\mathrm{r,\,IS}}$ obtained from KP and IS measurements were compared. For nonpolar octane, $\varepsilon^*_{\mathrm{r,\,KP}}$ was found to be nearly equal to $\varepsilon^*_{\mathrm{r,\,IS}}$. In contrast, for polar 1-octanol and 2-octanol, $\varepsilon^*_{\mathrm{r,\,KP}}$ and $\varepsilon^*_{\mathrm{r,\,IS}}$ were totally different. In octane, the agreement between $\varepsilon'_{\mathrm{r,\,KP}}$ and $\varepsilon'_{\mathrm{r,\,IS}}$ confirms the absence of an interface potential drop. However, in 1-octanol and 2-octanol, the smaller $\varepsilon'_{\mathrm{r,\,KP}}$ highlights the influence of space charge in reducing V_{bulk}. Potential profiles in liquid devices have remained largely unexplored, but this KP-based approach for evaluating energy diagrams offers a promising pathway to understanding the detailed mechanisms of polarization in liquids. This insight could significantly enhance the performance of electronics utilizing liquid-induced polarization. Furthermore, the target is not limited to liquids as long as it is deformable. If the frequency dependence can be measured analogously to the IS method, a more detailed evaluation of polarization characteristics will become feasible. Ongoing research aims to investigate such frequency-dependent behaviors, further refining this approach.

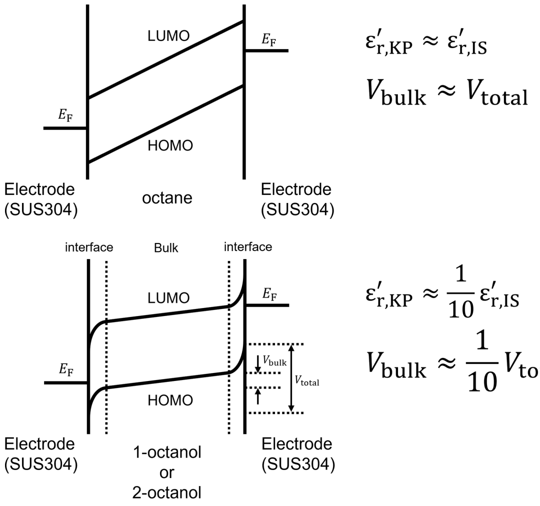

Figure 7. Evaluated energy diagrams of octane (upper) and 1-octanol or 2-octanol (lower) by comparing $\varepsilon'_{r,\,KP}$ and $\varepsilon'_{r,\,IS}$.

AUTHOR INFORMATION

Corresponding Authors

Haruto Jibiki − *Graduate School of Science and Engineering, Chiba University, Chiba 263-8522, Japan*; orcid.org/0009-0006-0281-689X; Email: jibikihrt@chiba-u.jp

Hisao Ishii − *Graduate School of Science and Engineering, Center for Frontier Science, and Molecular Chirality Research Center, Chiba University, Chiba 263-8522, Japan*; Email: ishii130@faculty.chiba-u.jp

Authors

Masato Suzuki − *Graduate School of Science and Engineering, Chiba University, Chiba 263-8522, Japan*

Masahiro Ohara − *Faculty of Engineering, Shinshu University, Nagano 390-8621, Japan*; orcid.org/0000-0001-5072-067X

Complete contact information is available at: https://pubs.acs.org/10.1021/acs.jpca.4c08604

Author Contributions

H.J. and M.S. constructed the measurement system with support from M.O. H.J. conducted the experiment and wrote the original manuscript. H.I. supervised, reviewed, and polished the manuscript.

Notes

The authors declare no competing financial interest.

ACKNOWLEDGMENTS

This research was financially supported by the Japan Society for the Promotion of Science (JSPS) KAKENHI Grant-in-Aid for Scientific Research (grant no. 24K01565).

ABBREVIATIONS

EDL, Electric double layer; IS, Impedance spectroscopy; KP, Kelvin Probe; KPFM, Kelvin Probe force microscopy; LIA, Lock-in amplifier

REFERENCES

(1) Dimitrakopoulos, C. D.; Purushothaman, S.; Kymissis, J.; Callegari, A.; Shaw, J. M. Low-Voltage Organic Transistors on Plastic Comprising High-Dielectric Constant Gate Insulators. *Science* **1999**, *283* (5403), 822−824.

(2) Huang, W.; Chen, J.; Wang, G.; Yao, Y.; Zhuang, X.; Pankow, R. M.; Cheng, Y.; Marks, T. J.; Facchetti, A. Dielectric Materials for Electrolyte Gated Transistor Applications. *J. Mater. Chem. C* **2021**, *9* (30), 9348−9376.

(3) Pei, Q.; Yu, G.; Zhang, C.; Yang, Y.; Heeger, A. J. Polymer Light-Emitting Electrochemical Cells. *Science* **1995**, *269*, 1086.

(4) Meier, S. B.; Tordera, D.; Pertegás, A.; Roldán-Carmona, C.; Ortí, E.; Bolink, H. J. Light-Emitting Electrochemical Cells: Recent Progress and Future Prospects. *Mater. Today* **2014**, *17* (5), 217−223.

(5) Urita, K.; Ide, N.; Isobe, K.; Furukawa, H.; Moriguchi, I. Enhanced Electric Double-Layer Capacitance by Desolvation of Lithium Ions in Confined Nanospaces of Microporous Carbon. *ACS Nano* **2014**, *8* (4), 3614−3619.

(6) Largeot, C.; Portet, C.; Chmiola, J.; Taberna, P.-L.; Gogotsi, Y.; Simon, P. Relation between the Ion Size and Pore Size for an Electric Double-Layer Capacitor. *J. Am. Chem. Soc.* **2008**, *130* (9), 2730−2731.

(7) Xing, W.; Qiao, S. Z.; Ding, R. G.; Li, F.; Lu, G. Q.; Yan, Z. F.; Cheng, H. M. Superior Electric Double Layer Capacitors Using Ordered Mesoporous Carbons. *Carbon* **2006**, *44* (2), 216−224.

(8) Petach, T. A.; Reich, K. V.; Zhang, X.; Watanabe, K.; Taniguchi, T.; Shklovskii, B. I.; Goldhaber-Gordon, D. Disorder from the Bulk Ionic Liquid in Electric Double Layer Transistors. *ACS Nano* **2017**, *11* (8), 8395−8400.

(9) Yuan, H.; Shimotani, H.; Tsukazaki, A.; Ohtomo, A.; Kawasaki, M.; Iwasa, Y. High-Density Carrier Accumulation in ZnO Field-Effect Transistors Gated by Electric Double Layers of Ionic Liquids. *Adv. Funct. Mater.* **2009**, *19* (7), 1046−1053.

(10) Xu, D.; Adachi, C. Organic Light-Emitting Diode with Liquid Emitting Layer. *Appl. Phys. Lett.* **2009**, *95* (5), No. 053304.

(11) Kubota, K.; Hirata, S.; Shibano, Y.; Hirata, O.; Yahiro, M.; Adachi, C. Liquid Carbazole Substituted with a Poly(Ethylene Oxide) Group and Its Application for Liquid Organic Light-Emitting Diodes. *Chem. Lett.* **2012**, *41* (9), 934−936.

(12) Hirata, S.; Kubota, K.; Jung, H. H.; Hirata, O.; Goushi, K.; Yahiro, M.; Adachi, C. Improvement of Electroluminescence Performance of Organic Light-Emitting Diodes with a Liquid-Emitting Layer by Introduction of Electrolyte and a Hole-Blocking Layer. *Adv. Mater.* **2011**, *23* (7), 889−893.

(13) Fort, T.; Wells, R. L. Measurement of Contact Potential Difference between Metals in Liquid Environments. *Surf. Sci.* **1968**, *12* (1), 46−52.

(14) Yee, S.; Oriani, R. A.; Stratmann, M. Application of a Kelvin Microprobe to the Corrosion of Metals in Humid Atmospheres. *J. Electrochem. Soc.* **1991**, *138* (1), 55.

(15) Macfadyen, K. A.; Holbeche, T. A. An Improved Technique for the Measurement of Contact Potential Differences. *J. Sci. Instrum.* **1957**, *34* (3), 101.

(16) Bastide, S.; Gal, D.; Cahen, D.; Kronik, L. Surface Photovoltage Measurements in Liquids. *Rev. Sci. Instrum.* **1999**, *70* (10), 4032−4036.

(17) Tsiplakides, D.; Archonta, D.; Vayenas, C. G. Absolute Potential Measurements in Solid and Aqueous Electrochemistry Using Two Kelvin Probes and Their Implications for the Electrochemical Promotion of Catalysis. *Top. Catal.* **2007**, *44* (3), 469−479.

(18) Hackl, T.; Schitter, G.; Mesquida, P. AC Kelvin Probe Force Microscopy Enables Charge Mapping in Water. *ACS Nano* **2022**, *16* (11), 17982−17990.

(19) Collins, L.; Kilpatrick, J. I.; Vlassiouk, I. V.; Tselev, A.; Weber, S. A. L.; Jesse, S.; Kalinin, S. V.; Rodriguez, B. J. Dual Harmonic Kelvin Probe Force Microscopy at the Graphene−Liquid Interface. *Appl. Phys. Lett.* **2014**, *104* (13), No. 133103.

(20) Collins, L.; Jesse, S.; Kilpatrick, J. I.; Tselev, A.; Okatan, M. B.; Kalinin, S. V.; Rodriguez, B. J. Kelvin Probe Force Microscopy in Liquid Using Electrochemical Force Microscopy. *Beilstein J. Nanotechnol.* **2015**, *6*, 201−214.

(21) Domanski, A. L.; Sengupta, E.; Bley, K.; Untch, M. B.; Weber, S. A. L.; Landfester, K.; Weiss, C. K.; Butt, H.-J.; Berger, R. Kelvin

Probe Force Microscopy in Nonpolar Liquids. *Langmuir* **2012**, *28* (39), 13892−13899.

(22) Umeda, K.; Kobayashi, K.; Oyabu, N.; Hirata, Y.; Matsushige, K.; Yamada, H. Practical Aspects of Kelvin-Probe Force Microscopy at Solid/Liquid Interfaces in Various Liquid Media. *J. Appl. Phys.* **2014**, *116* (13), No. 134307.

(23) Collins, L.; Jesse, S.; Kilpatrick, J. I.; Tselev, A.; Varenyk, O.; Okatan, M. B.; Weber, S. A. L.; Kumar, A.; Balke, N.; Kalinin, S. V.; et al. Probing Charge Screening Dynamics and Electrochemical Processes at the Solid−Liquid Interface with Electrochemical Force Microscopy. *Nat. Commun.* **2014**, *5* (1), 3871.

(24) Hirata, K.; Kitagawa, T.; Miyazawa, K.; Okamoto, T.; Fukunaga, A.; Takatoh, C.; Fukuma, T. Visualizing Charges Accumulated in an Electric Double Layer by Three-Dimensional Open-Loop Electric Potential Microscopy. *Nanoscale* **2018**, *10* (30), 14736−14746.

(25) Fumagalli, L.; Ferrari, G.; Sampietro, M.; Gomila, G. Dielectric-Constant Measurement of Thin Insulating Films at Low Frequency by Nanoscale Capacitance Microscopy. *Appl. Phys. Lett.* **2007**, *91* (24), No. 243110.

(26) Gramse, G.; Edwards, M. A.; Fumagalli, L.; Gomila, G. Dynamic Electrostatic Force Microscopy in Liquid Media. *Appl. Phys. Lett.* **2012**, *101* (21), No. 213108.

(27) Fumagalli, L.; Ferrari, G.; Sampietro, M.; Casuso, I.; Martínez, E.; Samitier, J.; Gomila, G. Nanoscale Capacitance Imaging with Attofarad Resolution Using Ac Current Sensing Atomic Force Microscopy. *Nanotechnology* **2006**, *17* (18), 4581.

(28) Kumar, B.; Crittenden, S. R. Nanoscale Dielectric Measurements from Electrostatic Force Microscopy. *Mod. Phys. Lett. B* **2014**, *28* (24), No. 1430011.

(29) Gramse, G.; Edwards, M. A.; Fumagalli, L.; Gomila, G. Theory of Amplitude Modulated Electrostatic Force Microscopy for Dielectric Measurements in Liquids at MHz Frequencies. *Nanotechnology* **2013**, *24* (41), No. 415709.

(30) Baikie, I.; Mackenzie, S.; Estrup, P.; Meyer, J. Noise and the Kelvin Method. *Rev. Sci. Instrum.* **1991**, *62* (5), 1326−1332.

(31) Dornte, R. W.; Smyth, C. P. THE DIELECTRIC POLARIZATION OF LIQUIDS. X. THE POLARIZATION AND REFRACTION OF THE NORMAL PARAFFINS. *J. Am. Chem. Soc.* **1930**, *52* (9), 3546−3552.

(32) Rauf, M. A.; Stewart, G. H.; Farhataziz. Viscosities and Densities of Binary Mixtures of 1-Alkanols from 15 to 55.Degree.C. *J. Chem. Eng. Data* **1983**, *28* (3), 324−328.

(33) Smyth, C. P.; Stoops, W. N. THE DIELECTRIC POLARIZATION OF LIQUIDS. VII. ISOMERIC OCTYL ALCOHOLS AND MOLECULAR ORIENTATION. *J. Am. Chem. Soc.* **1929**, *51* (11), 3330−3341.